

Developmental pathway of somatic embryogenesis in *Picea abies* as revealed by time-lapse tracking

Lada H. Filonova¹, Peter V. Bozhkov and Sara von Arnold

Department of Forest Genetics, Uppsala Genetic Centre, Swedish University of Agricultural Sciences, Box 7027, S-75007 Uppsala, Sweden

Received 1 June 1999; Accepted 1 October 1999

Abstract

Several coniferous species can be propagated via somatic embryogenesis. This is a useful method for clonal propagation, but it can also be used for studying how embryo development is regulated in conifers. However, in conifers it is not known to what extent somatic and zygotic embryos develop similarly, because there has been little research on the origin and development of somatic embryos. A time-lapse tracking technique has been set up, and the development of more than 2000 single cells and few-celled aggregates isolated from embryogenic suspension cultures of Norway spruce (*Picea abies* L. Karst.) and embedded in thin layers of agarose has been traced. Experiments have shown that somatic embryos develop from proembryogenic masses which pass through a series of three characteristic stages distinguished by cellular organization and cell number (stages I, II and III) to transdifferentiate to somatic embryos. Microscopic inspection of different types of structures has revealed that proembryogenic masses are characterized by high interclonal variation of shape and cellular constitution. In contrast, somatic embryos are morphologically conservative structures, possessing a distinct protoderm-like cell layer as well as embryonal tube cells and suspensor. The lack of staining of the arabinogalactan protein epitope recognized by the monoclonal antibody JIM13 was shown to be an efficient marker for distinguishing proembryogenic masses from somatic embryos. The vast majority of cells in proembryogenic masses expressed this epitope and none of cells in the early somatic embryos. The conditions that promote cell proliferation (i.e. the presence of exogenous auxin and cytokinin), inhibit somatic embryo formation; instead, continuous multiplication

of stage I proembryogenic masses by unequal division of embryogenic cells with dense cytoplasm is the prevailing process. Once somatic embryos have formed, their further development to mature forms requires abscisic acid and shares a common histodifferentiation pattern with zygotic embryos. Although the earliest stages of somatic embryo development comparable to proembryogeny could not be characterized, the subsequent developmental processes correspond closely to what occurs in the course of early and late zygotic embryogeny. A model for somatic embryogenesis pathways in *Picea abies* is presented.

Key words: *Picea abies*, proembryogenic mass, somatic embryo, time-lapse cell tracking.

Introduction

Plant embryogenesis begins with the zygote and passes through a stereotyped sequence of characteristic stages. Although considerable morphogenesis occurs after seed germination, the embryonic phase is crucial as it is here that the meristems and the shoot–root body pattern are specified.

In classical gymnosperm embryology, the whole embryogeny pathway comprises three phases (Singh, 1978): proembryogeny (stages before elongation of the suspensor), early embryogeny (stages after elongation of the suspensor and before establishment of the root meristem) and late embryogeny (establishment of the root and shoot meristems and further development of the embryo until maturity). A characteristic feature of gymnosperms is polyembryony manifested in the formation of more than one embryo in immature seed. Polyembryony sometimes results from the fertilization of more than one egg and the development of multiple zygotes (simple polyem-

¹ To whom the correspondence should be addressed. Fax: +46 18 67 32 79. E-mail: lada.filonova@sgen.slu.se

bryony). However, multiple embryos frequently form from a single zygote due to the cleavage of the embryonal mass into units that can develop further as individual proembryos (cleavage polyembryony). One proembryo is usually more vigorous and continues development while the others are aborted or absorbed by gametophytic tissue (Singh, 1978).

Because zygotic embryos are often difficult to isolate at particular stages after fertilization, detailed studies of the early embryonic development are hampered. This problem can be overcome by use of somatic embryos. In angiosperms, it has been shown that somatic embryos pass through a similar sequence of morphological stages as their zygotic counterparts (Mordhorst *et al.*, 1997). However, in conifers, very little is known about similarities and distinctions between somatic and zygotic embryogenesis, even though some exogenous factors ensuring formation of somatic embryos and subsequent plant regeneration have been described and incorporated in culture protocols (Attree and Fowke, 1993). For example, the continuous proliferation of embryogenic cultures requires auxin and cytokinin (Dong and Dunstan, 1994), whereas the further development and maturation of individual somatic embryos requires abscisic acid (ABA) (Dunstan *et al.*, 1998).

Despite the existence of successful protocols, the mechanism of proliferation in embryogenic cultures of conifers has not been followed in detail. Different mechanisms have been suggested (von Arnold and Hakman, 1988): (i) cleavage-like multiplication of somatic embryos; (ii) formation of somatic embryos through an asymmetrical division of a single cell or several such divisions within few-celled aggregates; (iii) direct formation of new somatic embryos from small meristematic cells within suspensor-like cells.

The successive developmental stages leading to establishment of the mature somatic embryo must be understood fundamentally for optimal management of somatic plant regeneration systems. Ideally, this task has to be accomplished by construction of a fate map of somatic embryogenesis, which, as in other developmental processes, includes an adequate number of morphological and molecular markers specifying distinct stages within the whole process (Irish and Sussex, 1992; Strehlow and Gilbert, 1993). Furthermore, when constructed, the fate map showing the correct progression of somatic embryogenesis would facilitate further efforts to analyse gene expression at particular stages of embryo development and to identify mutant forms.

Construction of a fate map in somatic embryogenesis can be based on two alternative approaches: (i) using synchronous cell-division systems (Nomura and Komamine, 1985; Tsukahara and Komamine, 1997), or (ii) by time-lapse tracking of development of individual protoplasts, cells and multicellular structures (Backs-Hüsemann and Reinert, 1970; Golds *et al.*, 1992; Toonen

et al., 1994). Carrot (*Daucus carota*) is the only species where both approaches have been successfully employed (Zimmerman, 1993; Mordhorst *et al.*, 1997).

The aim of this work is to develop a model for explaining how somatic embryos of a conifer, Norway spruce, proliferate and develop, and to analyse whether or not these embryos pass through the same sequence of steps characteristic of zygotic embryogenesis. A time-lapse tracking technique has been set up, and the development of more than 2000 single cells and few-celled aggregates has been traced.

Materials and methods

Cell culture

Six embryogenic cell lines of Norway spruce (*Picea abies* L. Karst.) were used throughout this study. They were established in different years from immature zygotic embryos as previously described (Egertsdotter and von Arnold, 1993). Three of the cell lines, A95.88.17, A95.88.22 and A95.88.25, were of A-type and produced predominantly normal mature somatic embryos in response to ABA. Three other cell lines were considered as B-type. Two of them, B41 and B45, produced only abnormal cotyledonary embryos possessing a shortened and swollen hypocotyl, which were unable to germinate, whereas cell line B88.1 displayed no signs of somatic embryo development at all and continued to proliferate under ABA-treatment (Egertsdotter and von Arnold, 1993, 1998). These patterns of response to ABA were rather stable and did not change in the course of the present study.

All six cell lines were cultured under standard conditions for 3 months prior to the onset of the experiments. Briefly, every week during subculturing, 2 ml of densely packed cells were transferred to 48 ml liquid fresh proliferation medium (i.e. 4% starting settled cell volume) in 250 ml Erlenmeyer flasks. Cultures were grown on a gyratory shaker (100 rpm) in darkness at $22 \pm 1^\circ\text{C}$.

For the morphological assessment, cell cultures were first incubated for 8 min with 1% (w/v) acetocarmine followed by brief (less than 1 min) counterstaining with 0.05% (w/v) Evan's blue.

The proliferation medium used for both maintenance of cell lines and time-lapse tracking experiments consisted of half-strength LP (von Arnold and Eriksson, 1981) macro- and micro-salts, monosaccharides and vitamins, 30 mM sucrose, 3.0 mM L-glutamine (filter-sterilized into autoclaved cooled medium), 9.0 μM 2,4-dichlorophenoxyacetic acid (2,4-D) and 4.4 μM N⁶-benzyladenine (BA). The pH was adjusted to 5.8 ± 0.1 prior to autoclaving.

The basal maturation medium employed for the tracking of individual somatic embryo development and maturation was full-strength BMI-S1 (Krogstrup, 1986) supplemented with 88 mM sucrose, 5.5 mM myo-inositol and 500 mg l⁻¹ casein hydrolysate (pH 5.8 ± 0.1 , adjusted prior to autoclaving). L-glutamine (3.0 mM) and ABA (30 μM) were filter-sterilized into autoclaved cooled medium.

Fractionation of cell cultures and cell tracking

The 3-d-old cell suspensions were sieved through 200 μm nylon mesh, and the $>200 \mu\text{m}$ fraction resuspended in proliferation medium. This procedure enabled dissociation of adhered cell aggregates. The resulting cell suspension greater than 200 μm was then passed through a series of meshes with successive 600,

400, 200, and 80 µm pore sizes. Single cells and few- and multi-celled aggregates were obtained from the <80, 200–400, and 400–600, µm fractions, respectively. Unless otherwise stated, these fractions were inoculated into either 0.5 or 1.5 ml aliquots of liquid proliferation medium held in 24 well plates (Nunc, Denmark) or 60 mm Petri dishes (Sarstedt, NC, USA), respectively. The fractions inoculated in 24 well plates represented non-immobilized treatment, whereas those inoculated in Petri dishes were subsequently immobilized by mixing with the same volumes of 1.2% (w/v) Seaplaque agarose (FMC BioProducts, Rockland, USA)-containing proliferation medium at 35 °C. In either type of culture the plating density was set at 25–30 cells or aggregates ml⁻¹. The cultures were incubated in the darkness at 22 ± 1 °C.

Most of the cell-tracking experiments were done in thin layers of agarose. The nutrient composition of agarose layers was replenished every 2 weeks through gentle addition and removal of three 5 ml aliquots of proliferation medium lacking 2,4-D and BA.

To stimulate individual somatic embryo development, the proliferation medium was replaced after 50–60 d through 6 step washing of agarose layers by 5 ml aliquots of maturation medium. Further replenishment of agarose layers was achieved by weekly addition and removal of three 5 ml aliquots of ABA-containing medium.

The whole developmental pathway, from individual preselected single cells or few-celled aggregates to mature somatic embryos, was tracked using an inverted microscope (Axiovert 10, Zeiss, Germany). To pinpoint a particular cell or aggregate, the microscope stage was equipped with a circle of transparency film (diameter 50 mm) ruled into numbered 5 × 5 mm squares. When placed on the microscope stage, the bottom of the Petri dish was superimposed on this circle. Preselected developing cells or aggregates were photographed daily on AGFAPAN APX-25 film and their images were simultaneously recorded on a Panasonic WVP-F10E video camera (Matsushita Co., Japan) equipped with a video graphic printer UP-811 (Sony, Japan).

Histological preparations

Samples were taken from proliferating suspension cultures, 3 d and 7 d after subculture, as well as from some agarose layers that were used as a source of developmental stages only for histological analysis. In the latter case, small aggregates were cut from agarose layers leaving enough agarose around to protect aggregates from injury during fixation and embedding. Somatic embryos at late developmental stages were gently extracted from agarose layers with forceps. Sampling was done every day during the first 5 d in proliferation medium, and then every 5 d until mature somatic embryos had formed.

The samples were sequentially fixed, first in 0.5% (w/v) paraformaldehyde and 0.75% (v/v) glutaraldehyde for 1 h, and second in 1% paraformaldehyde and 1.5% glutaraldehyde for 2 h. Both fixation solutions were prepared in 0.1 M sodium phosphate buffer (PBS), pH 7.0, with the addition of a drop of Tween 20. Thereafter, the embryos were dehydrated slowly in a graded ethanol series (from 70 to 100%, 30 min per step) followed by the gradual replacement of absolute ethanol by Technovit 7100 (Kulzer, Germany), 2:1, 1:1, 1:2 (v/v) ethanol:Technovit (30 min per step) and pure Technovit overnight. All the steps except the last one were performed under a slight vacuum at 20 °C (last step at 4 °C). Finally, the material was embedded in fresh Technovit and sectioned on a motorized microtome (HM 350, Microm, Germany). The sections (3 µm) were placed on poly-L-lysine coated slides (Menzel-Glaser, Germany) and were stained with toluidine blue

and examined through a light microscope (Axioplan, Zeiss, Germany). The sections were photographed on Kodak Ektachrome 160T film.

Immunocytochemistry

Samples for immunocytochemistry were collected and fixed as described for histological preparations. The dehydration, infiltration and embedding procedure has been described previously (Gubler, 1989; Baskin *et al.*, 1992) and was modified as follows. Samples were dehydrated to 100% ethanol at 30 min intervals, 50, 70% at 20 °C and 90, 100% at 4 °C. Dithiothreitol (DDT; Sigma, MO, USA) was added to the ethanol series from 50 to 90% and to the absolute ethanol at concentrations 1 and 10 mM, respectively. Then samples were infiltrated through an ethanol-methacrylate series, 2:1, 1:1, 1:2 (v/v) ethanol:methacrylate and left in pure methacrylate overnight (all steps at 4 °C). A slight vacuum was applied at all steps except for the last one. The methacrylate mixture contained 4:1 (v/v) butylmethacrylate (Acros Organics, NJ, USA) to methylmethacrylate (Sigma, MO, USA), 0.5% (w/v) benzoin ethyl ether (Sigma, MO, USA) and 10 mM DTT. The mixture was degassed by bubbling helium through for 15 min.

Before embedding, the samples were placed in fresh methacrylate mixture for 1 h under slight vacuum at 4 °C followed by transfer to gelatin capsules (NR0, ACL Kval E, Apoteksbolaget, Göteborg, Sweden), each containing 300 µl of fresh pure methacrylate. Polymerization was performed in an aluminium box (215 × 215 × 145 mm) under long-wave UV light (KeboLab, Sweden) at 4 °C for about 4 h.

The primary antibody for immunocytochemistry was JIM13, raised against a specific epitope of arabinogalactan proteins (AGPs) present in carrot cell walls (Knox *et al.*, 1991). For antibody labelling, sections of 2–4 µm, prepared as described for histological preparations, were treated as follows: 15 min in pure acetone (to remove resin); rehydration in decreasing ratios of ethanol (100, 80, 50 and 30%, 1 min each); three rinses in PBS (10 min each); 20 min in PBS with 1% (v/v) calf serum (ICN Biomedicals, CA, USA); overnight at 4 °C in JIM13 monoclonal antibody culture supernatant (kindly provided by Dr K Roberts, John Innes Institute, Norwich, UK) diluted 1:50 in PBS and supplemented with 2% calf serum and 0.1% (v/v) Tween 20; three washes (30 min each) in PBS on a magnetic stirrer; treatment by secondary antibody, goat anti-rat IgG antiserum conjugated to FITC (goat anti-rat IgG-FITC; Calbiochem, CA, USA), diluted 1:500 in PBS with 2% calf serum and 0.1% Tween 20 for 1 h in darkness; three final rinses in PBS (10 min each) followed by 10 min treatment with 0.25% Evan's blue (to reduce autofluorescence). Processed sections were mounted in Fluorsave (Calbiochem, CA, USA) and covered by coverslips. To check the specificity of JIM 13-immunolabelling, duplicate sections were treated only with goat anti-rat IgG-FITC and Evan's blue. Immunostained sections were examined through an Axioplan (Zeiss, Germany) microscope, equipped with an HBO 50W mercury short arc lamp (OSRAM, Germany), epifluorescence optics, and the standard set of filters for FITC. Kodak Elite II 400 film was used for photomicrography. Non-labelled duplicate sections stained with toluidine blue served as a morphological control and were examined as for histological analysis.

Results

Characterization of embryogenic suspension cultures

Embryogenic cell lines of *P. abies* have previously been divided into two groups, A and B (Egertsdotter and von

Arnold, 1993, 1995; Egertsdotter *et al.*, 1993; Mo *et al.*, 1996). Only somatic embryos belonging to A-group cell lines mature normally in response to ABA. For group B cell lines, there are two alternative situations. Some cell lines never reach the developmental stage required for maturation in response to ABA; instead, they proliferate continuously without any signs of cotyledonary embryo formation. However in the other type of cell line within group B embryos do develop in response to ABA, but the cotyledonary somatic embryos are always abnormal and unable to germinate. In accordance with this classification, cell lines representing all three categories were analysed: A95.88.22 (normal mature somatic embryos), B88.41 (abnormal cotyledonary somatic embryos) and B88.1 (no cotyledonary somatic embryos). The results presented below have been confirmed with three additional cell lines: A95.88.17, A95.88.25 and B88.45 (data not shown).

All embryogenic cell lines are composed of two types of cells, i.e. highly vacuolated cells, which are more or less elongated, and rounded densely cytoplasmic cells. These cells differ in affinity for staining with acetocarmine and Evan's blue: the densely cytoplasmic cells stain bright red with acetocarmine, whereas highly vacuolated cells are permeable to Evan's blue. The majority of cells are clustered into aggregates of different size and form which vary among cell lines (Fig. 1). These aggregates present in proliferating embryogenic cultures have been designated proembryogenic masses (PEMs). Three stages were

distinguished, based on morphology as well as on developmental pattern: PEM I, PEM II and PEM III. At stage PEM I, a cell aggregate is composed of a small compact clump of densely cytoplasmic cells adjacent to a single vacuolated cell showing a tendency to elongation in A-type cell lines (Fig. 1). Similar cell aggregates which possess more than one vacuolated cell were classified as PEM II (Figs 1, 2A). At stage PEM III, an enlarged clump of densely cytoplasmic cells appears loose rather than compact; polarity is disturbed (Figs 1; 2B, C). Histological analysis has shown that, in contrast to somatic embryos, PEMs lack a distinct embryonal mass, protoderm-like layer and embryonal tube cells (Fig. 2).

Time-lapse tracking of somatic embryo formation

Development of more than 2000 single cells and PEMs obtained from five embryogenic cell lines (cell line 88.1 showing no signs of somatic embryo formation was excluded from the analyses) was monitored by a time-lapse tracking technique. Three-day-old suspensions were passed through a series of sieves with successive 600, 400, 200, and 80 μ m pore sizes. Most of the single cells that passed through the 80 μ m pore size started to divide, but they never developed further into PEMs and somatic embryos.

Proembryogenic masses I collected from the top of the 200 μ m sieve were immobilized in thin layers of agarose and their developmental pathway was recorded. Tracking

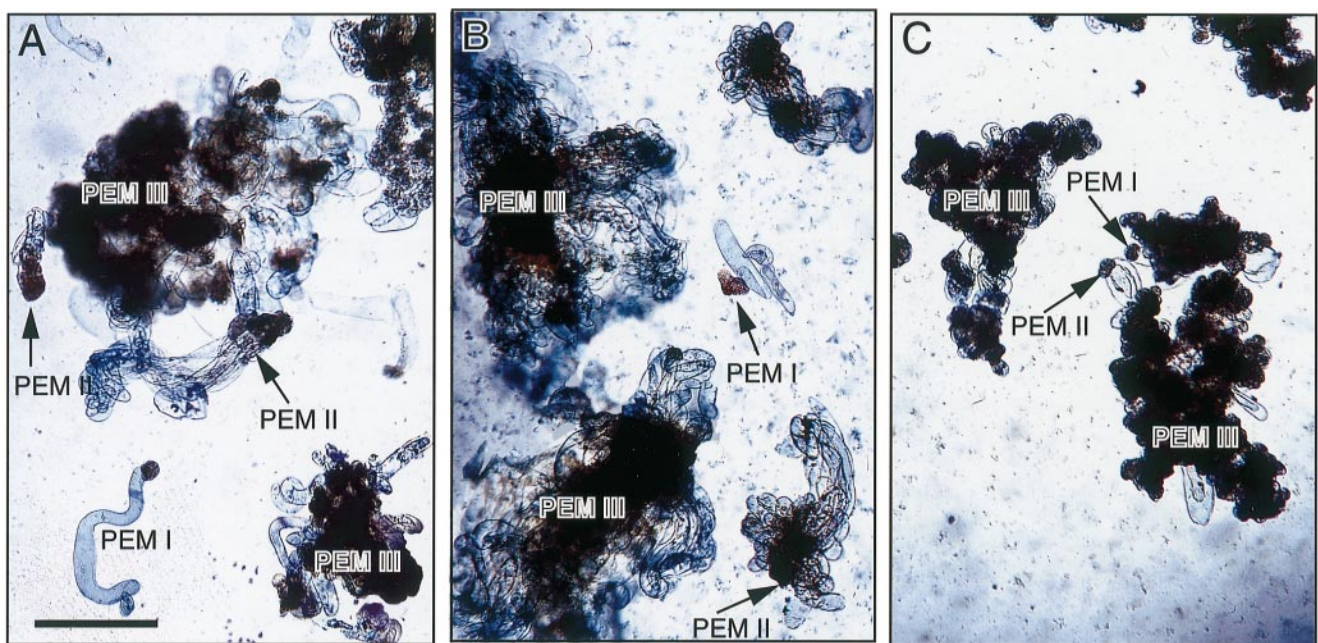


Fig. 1. Overview of embryogenic suspension cultures in proliferation medium. Samples were taken 3 d after subculture and stained with acetocarmine and Evan's blue. Cell aggregates with varying morphology are designated proembryogenic masses and classified as stages PEM I, PEM II and PEM III. (A) Cell line A95.88.22 producing predominantly normal mature somatic embryos on maturation medium. (B) Cell line B41 producing abnormal cotyledonary somatic embryos on maturation medium. (C) Cell line B88.1 producing no somatic embryos on maturation medium. Bar = 250 μ m.

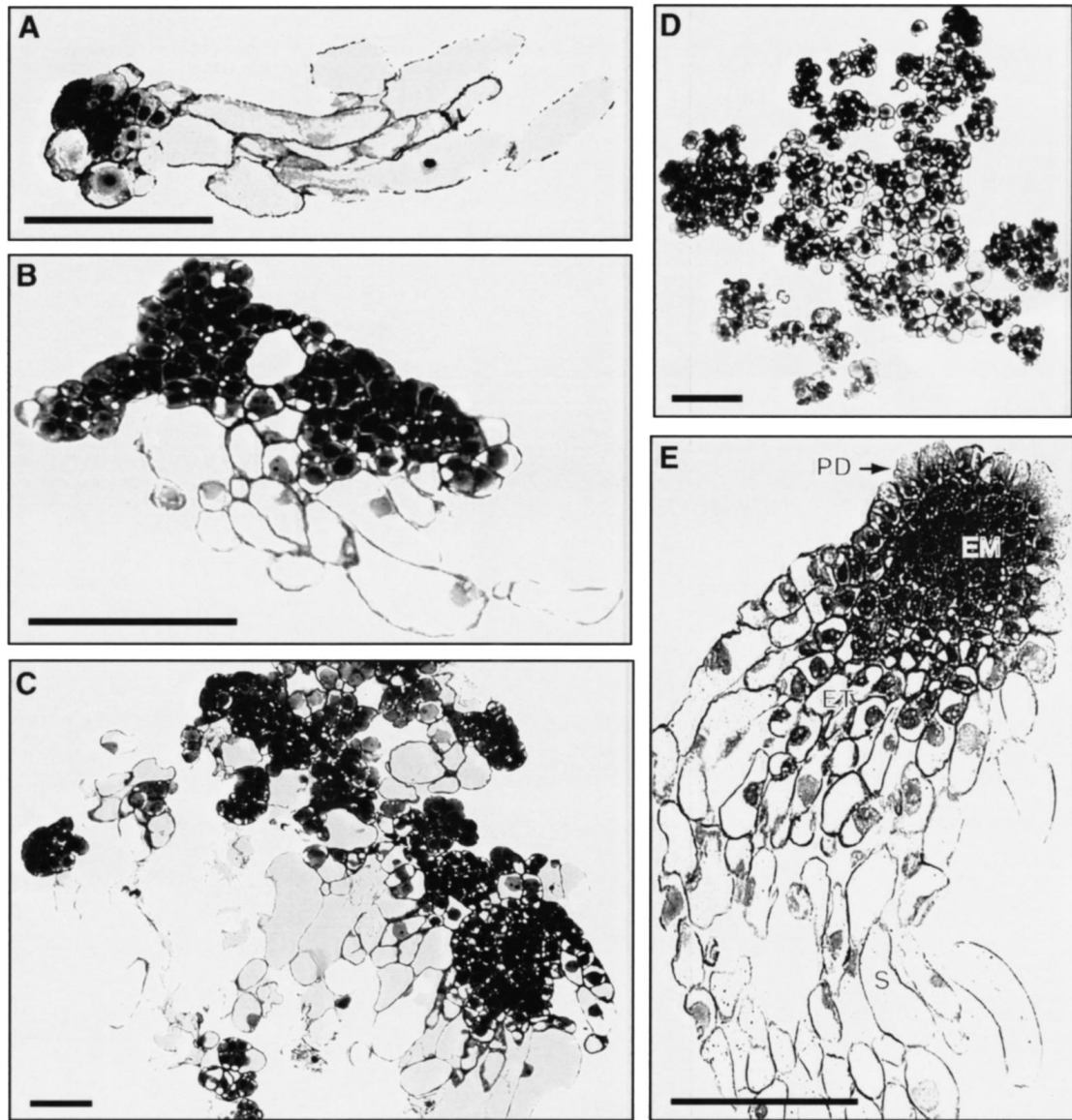


Fig. 2. Histological features of PEMs compared to somatic embryos. Samples were taken from proliferating suspension cultures, 3 d after subculture for PEMs and 7 d for somatic embryos. The sections were stained with toluidine blue. (A, B) PEM II and PEM III, respectively, both containing two types of cells, rounded densely cytoplasmic and elongated or oval highly vacuolated (cell line A95.88.22). The polarity of PEM III appears disturbed compared to PEM II. (C) A lobing-like proliferation at PEM III level (cell line B41). (D) Non-polarized PEMs lacking elongated cells (cell line B88.1). (E) Early somatic embryo possessing embryonal mass (EM), protoderm-like layer (PD), embryonal tube cells (ET) and suspensor (S) (cell line A95.88.22). Bars = 250 µm.

of the development of 47 PEMs I from three different A-group cell lines has shown the same developmental pathway. An example is shown in Fig. 3. No remarkable changes occurred within the first 2 d (Fig. 3A, B). The highly vacuolated elongated cell had elongated further and the compact clump of densely cytoplasmic cells had expanded through new divisions. At day 3, additional elongated cells had developed from the compact clump of densely cytoplasmic cells, thereby forming what was defined as a PEM II (Fig. 3C). Evan's blue staining intensity of the primary vacuolated elongated cell increased by day 3 and was higher compared to newly

formed additional vacuolated cells (not shown). Successively PEM II enlarged in size by producing more cells of both types, while maintaining a bipolar pattern (Fig. 3D–F). The polarity and the distinct centre of densely cytoplasmic cells were lost after day 10 owing to the increased proliferative activity of densely cytoplasmic cells. This process continued from day 15 onward leading to formation of PEM III (Fig. 3G, H), followed by transdifferentiation of somatic embryos from PEM III (Fig. 3I–K). Several somatic embryos often formed from a single PEM III.

Tracking of development of 40 PEMs I belonging to

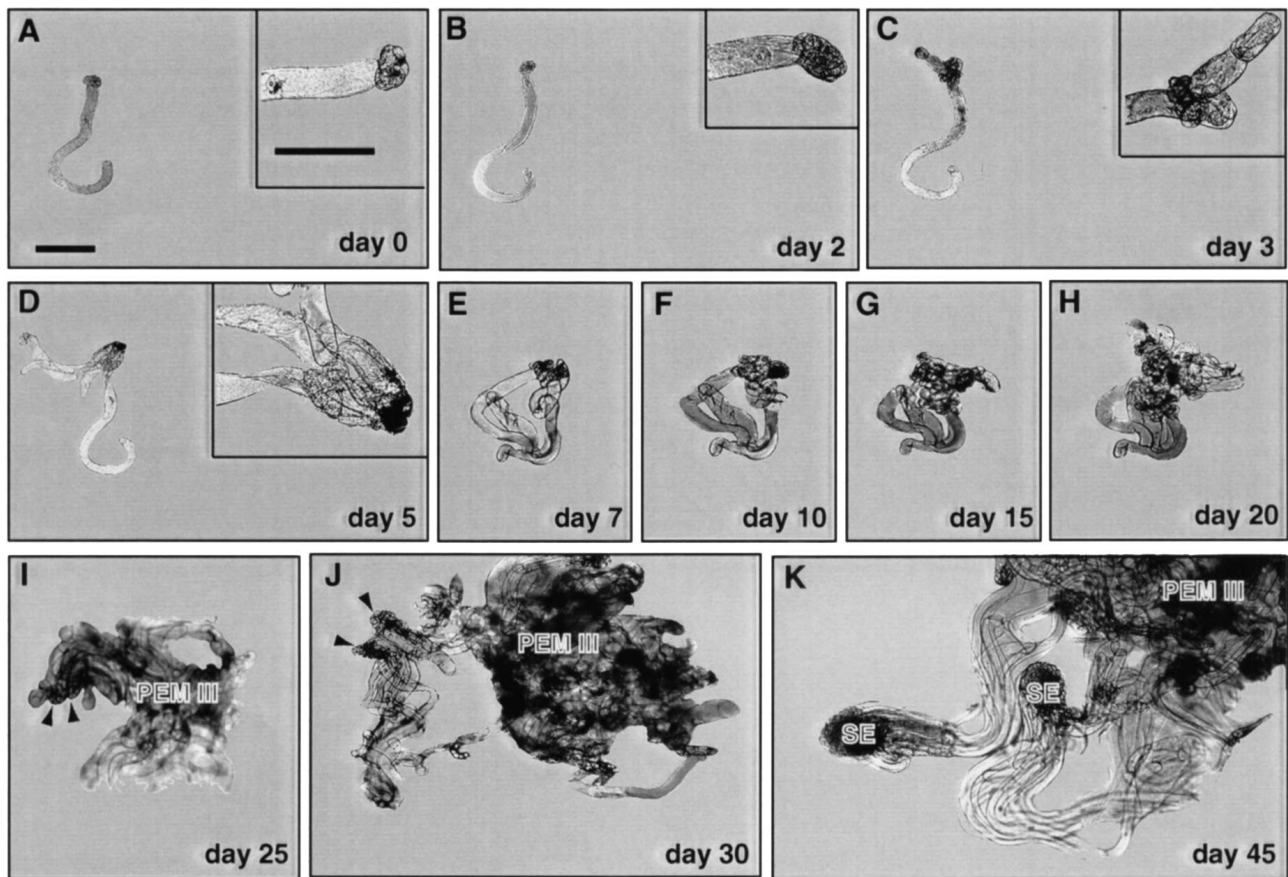


Fig. 3. Developmental pathway leading to somatic embryo formation in A-type cell line A95.88.22. A 3-d-old cell suspension was passed through a series of sieves with successive 600-, 400- and 200 μm pore sizes. Individual few-celled aggregates were collected from the top of the 200- μm sieve and immobilized in thin layers of agarose (density 25–30 aggregates ml^{-1}) containing proliferation medium. The nutrient composition of agarose layers was replenished every 2 weeks. Tracking was run for 45 d. Microscopic images were recorded at days 0 (A), 2 (B), 3 (C), 5 (D), 7 (E), 10 (F), 15 (G), 20 (H), 25 (I), 30 (J), and 45 (K). Arrowheads denote somatic embryos transdifferentiating from PEM III. SE, somatic embryo. The figure is a representative example of 47 whole tracks recorded. Bars = 250 μm .

two B-type cell lines has revealed the common pathway. An example is presented in Fig. 4. No fundamental differences in the development of PEM I from group A and group B cell lines were observed. However, along with polar PEMs I, similar to those characteristic of A-cell lines (Fig. 3A), PEMs I lacking strict polarity were common in B-lines as well. The latter had loose aggregates of small densely cytoplasmic cells adjacent to an enlarged highly vacuolated cell (Fig. 4A). Both types of PEM I were found in every B-type cell suspension. Additional vacuolated cells developed during the first 5 d (Fig. 4B–E). At PEM II stage, high rates of multiplication of both types of cell led to a pronounced increase in the size of the whole aggregate, and a highly polarized morphology was established by day 25 (Fig. 4F–J). At day 30, new PEM formed from enlarged PEM II (Fig. 4K). The newly developed PEM had a similar morphology as the original 2-d-old PEM II (Fig. 4B cf. K). Further growth of PEM II led to acquisition of PEM III structural characteristics by day 35 (Fig. 4L–O).

Transdifferentiation of somatic embryos occurred by days 50–60 coincident with the development of strictly polar PEM II from newly formed PEM (Fig. 4O, P). Several somatic embryos formed from a single PEM III.

Time-lapse tracking of somatic embryo development and maturation

For further somatic embryo development and maturation, ABA must be supplied continuously. This was accomplished by replacing the proliferation medium in agarose layers with the ABA-containing medium (see Materials and methods).

The first visible response of A and B-type early somatic embryos to ABA was detected at day 4, when embryonal masses became opaque (Figs 5A, 6A). In the A-type, this response was accompanied by degradation of the suspensor-like cells (not shown). Thereafter A-embryos started to elongate (Fig. 5B–D). Cotyledon formation occurred 18–20 d after addition of ABA (Fig. 5E). In

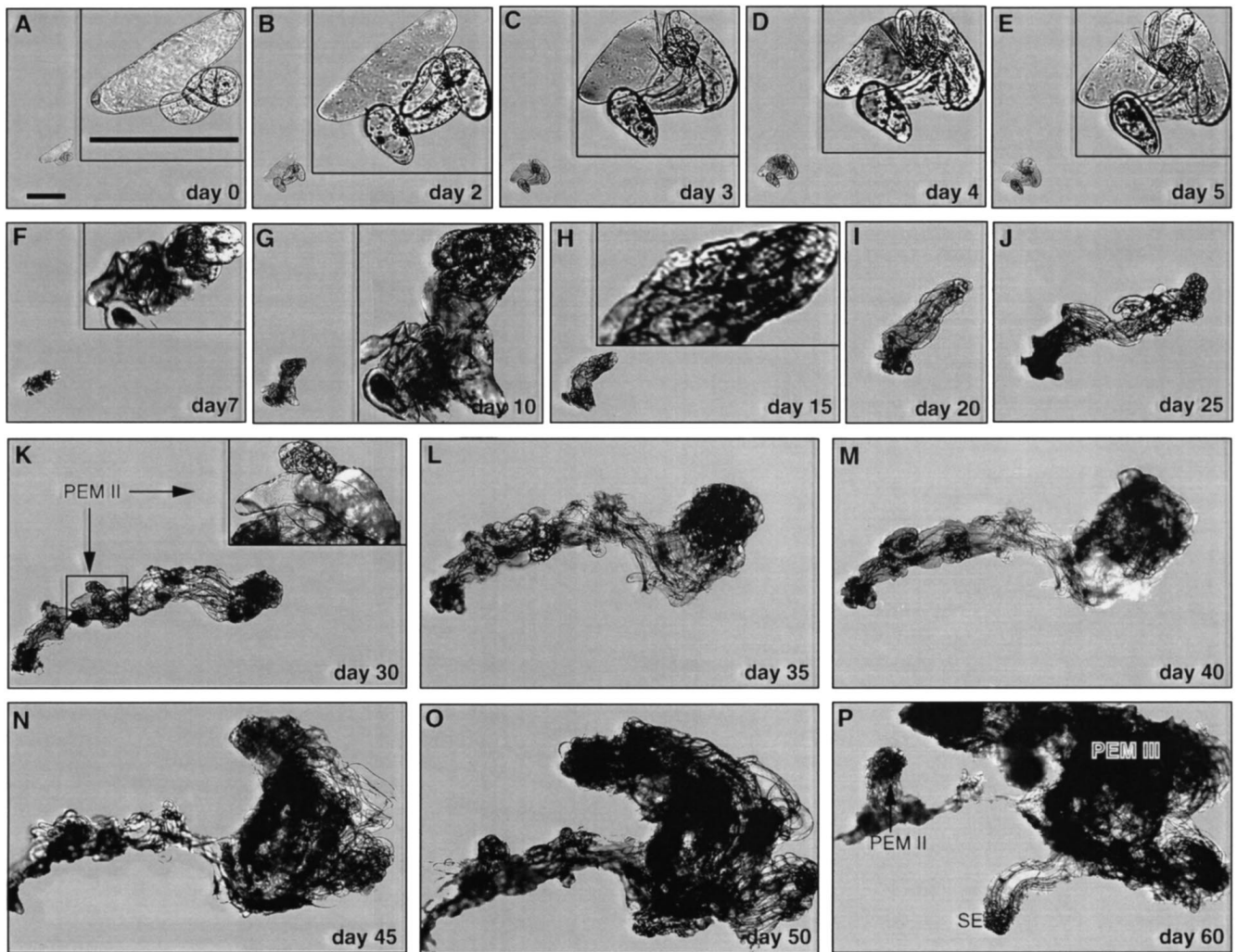


Fig. 4. Developmental pathway leading to somatic embryo formation in B-type cell line B41. For structure selection and immobilization procedures see legend to Fig. 3. Tracking was run for 60 d. Microscopic images were recorded at days 0 (A), 2 (B), 3 (C), 4 (D), 5 (E), 7 (F), 10 (G), 15 (H), 20 (I), 25 (J), 30 (K), 35 (L), 40 (M), 45 (N), 50 (O), and 60 (P). Note the lack of strict polarity of PEM I and that small densely cytoplasmic cells are more loosely packed than in the A-type pathway (A–E cf. Fig. 3A, B). The newly formed PEM II in (K) is enclosed in a box. SE, somatic embryo. The figure is a representative example of 40 whole tracks recorded. Bars = 250 μ m.

contrast to A-embryos, B-embryos demonstrated greater longevity of suspensor-like cells (Fig. 6B–D) with the first signs of their degradation detected at day 20 (Fig. 6E). Furthermore, B-embryos showed intensive radial growth during the whole process of maturation (Fig. 6E–H). Cotyledon formation occurred after 30–35 d of ABA treatment (Fig. 6G). Matured somatic embryos exhibiting different morphology between A- and B-group cell lines formed after 45 d of ABA treatment (Figs 5H, 6H).

Histological analysis showed that early somatic embryos of A-lines had a globular compact embryonal mass, with a distinct protoderm-like layer, a layer of embryonal tube cells, and suspensor-like cells (Fig. 7A). The suspensor-like cells degenerated shortly after addition of ABA (Fig. 7B). In contrast, the embryonal mass

of early B-embryos lacked a protoderm-like layer (Fig. 8A), which differentiated following addition of ABA (Fig. 8B).

At the beginning of late embryogeny, somatic embryos of A-lines established the root-organization centre (Fig. 7C). Most visible histogenesis occurred in the middle of late embryogeny. By the time of cotyledon formation, somatic embryos had passed through all the steps of histogenesis. The root meristem was located in the basal part of somatic embryo, owing to active proliferation of embryonal cortex cells adjacent to the procambium. Somatic embryos had well-developed pith and shoot apex (Fig. 7D). An A-type embryo enlarged predominantly in the axial direction.

The shape of somatic embryos from B-lines in the middle of late embryogeny was rounded rather than

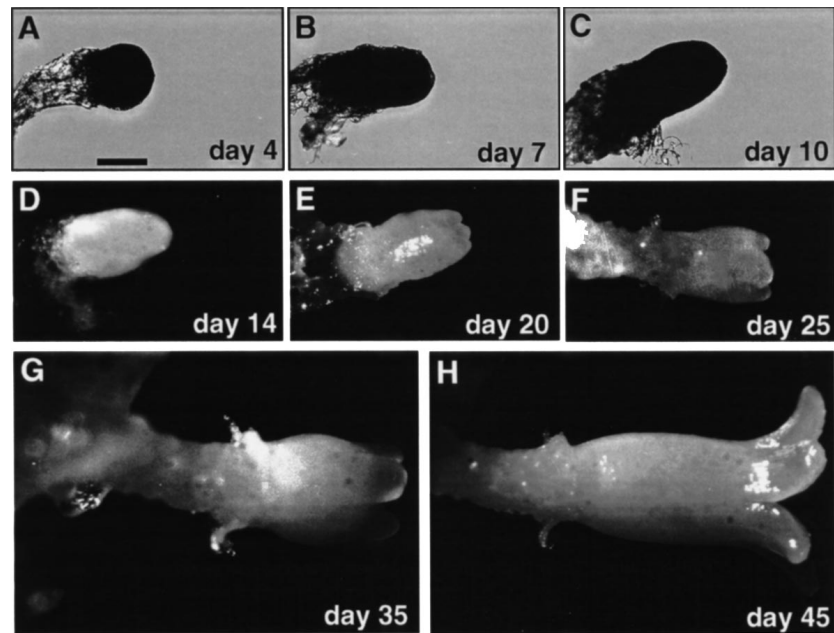


Fig. 5. Somatic embryo development in A-type cell line A95.88.22. Proliferation medium in thin layers of agarose was replaced by ABA-containing maturation medium, which was subsequently replenished at weekly intervals. Microscopic images were recorded at days 4 (A), 7 (B), 10 (C), 14 (D), 20 (E), 25 (F), 35 (G), and 45 (H). The figure is a representative example of 10 whole tracks recorded. Bar = 250 μ m.

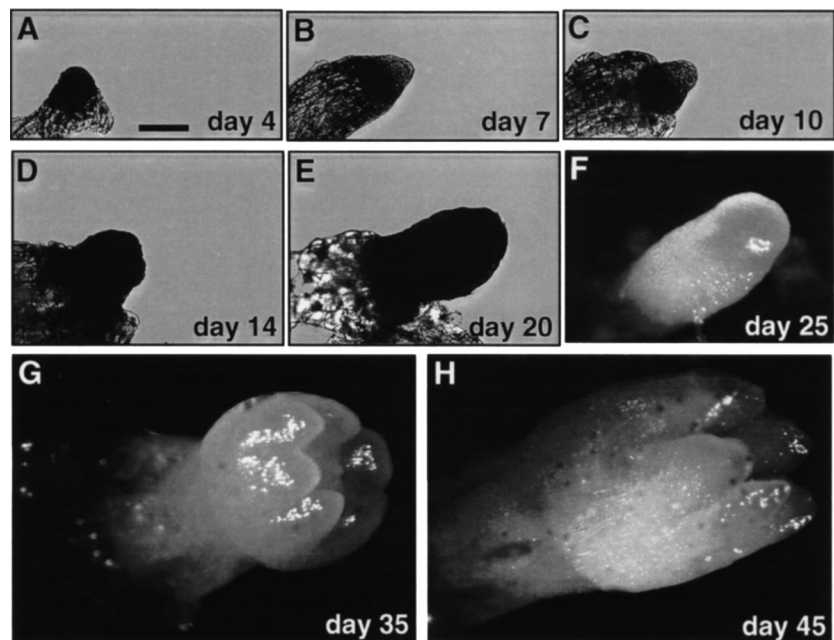


Fig. 6. Somatic embryo development in B-type cell line B41. Proliferation medium in thin layers of agarose was replaced by ABA-containing maturation medium, which was subsequently replenished at weekly intervals. Microscopic images were recorded at days 4 (A), 7 (B), 10 (C), 14 (D), 20 (E), 25 (F), 35 (G), and 45 (H). The figure is a representative example of 12 whole tracks recorded. Bar = 250 μ m.

elongated, and the onset of histogenesis was still not evident (Fig. 8C). At the end of late embryogeny, somatic embryos were already differentiated, and the width of the embryo approximated its length (Fig. 8D). The root meristem was located closer to the shoot apex than in the A-type embryo counterpart (Figs 7D cf. 8D).

After cotyledon formation, B-type embryos expanded in both radial and axial directions. Additionally embryonal tissues were disrupted, with air spaces forming within the shoot apex region (Fig. 8E), and ultimately, pith and cortex degenerating (Fig. 8F). Such B-embryos were unable to germinate.

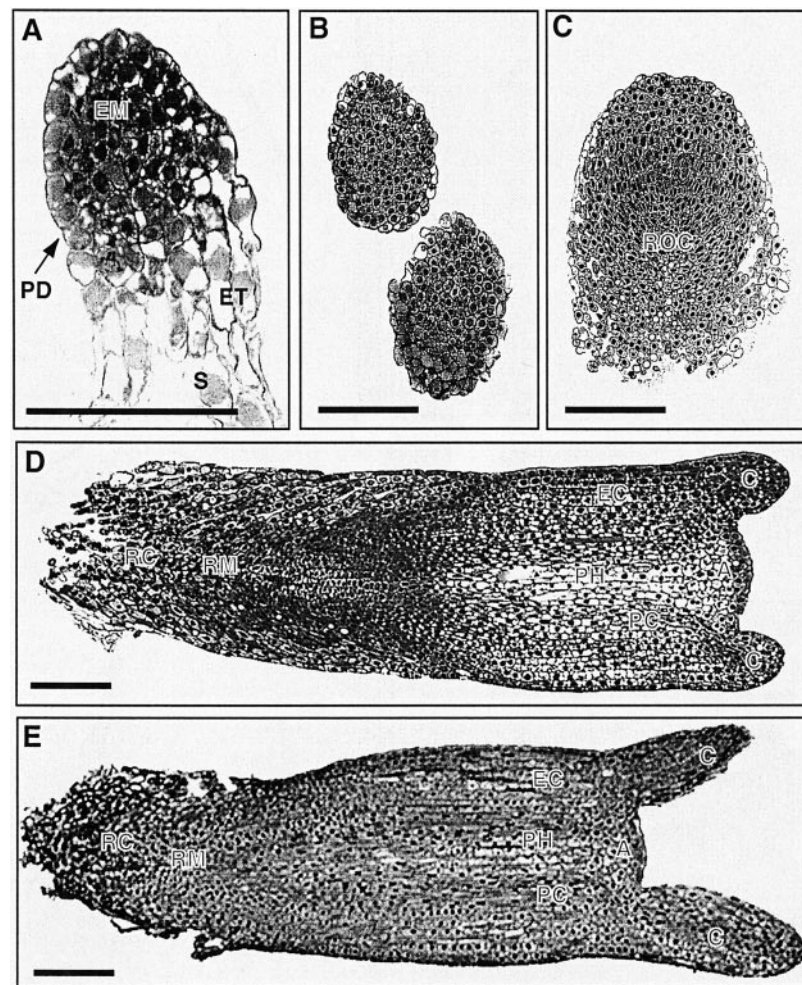


Fig. 7. Histology of somatic embryo development in A-type cell line A95.88.22. The longitudinal sections were stained with toluidine blue. (A) Early somatic embryo possessing embryonal mass (EM) with protoderm-like layer (PD), embryonal tube cells (ET) and suspensor-like cells (S). The embryo is developmentally comparable to those shown in Fig. 3K. (B) Somatic embryo at the end of early embryogenesis (developmentally comparable to that shown in Fig. 5B). (C) Somatic embryo in the beginning of late embryogenesis (developmentally comparable to that shown in Fig. 5D). ROC, root-organization centre. (D) Somatic embryo at the end of late embryogenesis (developmentally comparable to that shown in Fig. 5G). Root meristem (RM) participating in root cap (RC) formation is located in the basal part of somatic embryo, owing to active proliferation of embryonal cortex (EC) cells adjacent to procambium (PC). A, shoot apex; C, cotyledons; PH, pith. (E) Mature somatic embryo (developmentally comparable to that shown in Fig. 5H). Bars = 250 µm.

Development of proembryogenic masses and somatic embryos under different environments

The predominant response of PEMs placed at low density in well-aerated liquid medium with high levels of auxin and cytokinin (molar ratio 2:1) was unequal division of embryogenic cells with dense cytoplasm leading to the restart of the process from the PEM I level (Fig. 9). Therefore, under these conditions the whole system is determined to remain at the PEM I level.

Immobilization of PEMs in the presence of exogenously supplied auxin and cytokinin permitted both multiplication by new PEM I formation and successive growth to more advanced levels (PEM I to PEM II and PEM II to PEM III; Fig. 9). It is notable that even partial aggrega-

tion of structures in liquid medium, when cell density is high enough, led to successive development of PEM I into PEM II, PEM II into PEM III, and sometimes to transdifferentiation of PEM III to somatic embryos (data not shown).

The early somatic embryos subjected to auxin and cytokinin always reinitiated the embryogenic process through proliferation in embryonal mass, irrespective of whether or not immobilization was applied (Fig. 9).

Abscisic acid inhibited PEM proliferation and growth for the majority of cell lines; PEMs I and PEMs II usually died in response to ABA. The main developmental effect of ABA was transdifferentiation of PEMs III to somatic embryos followed by individual somatic embryo development (Fig. 9). The cleavage of early somatic embryos

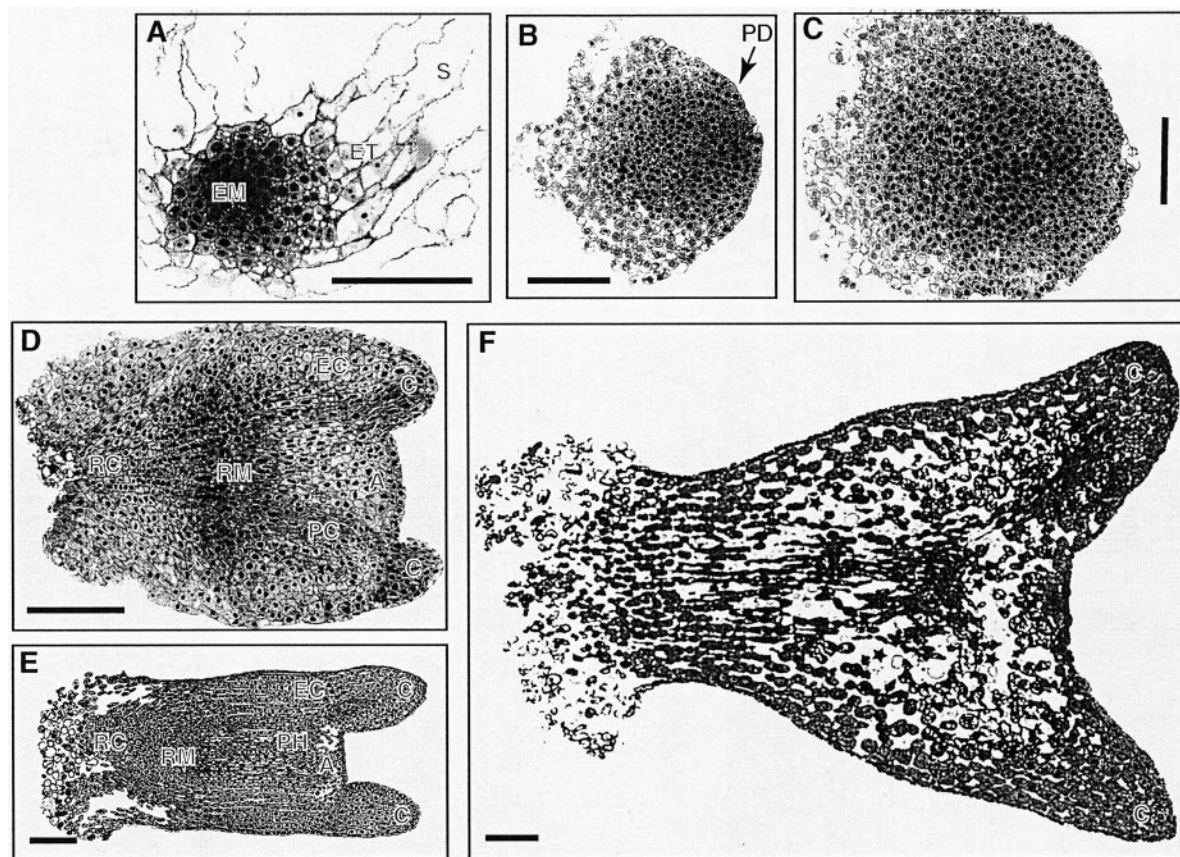


Fig. 8. Histology of somatic embryo development in B-type cell line B41. The longitudinal sections were stained with toluidine blue. (A) Early somatic embryo with embryonal mass (EM), embryonal tube cells (ET) and suspensor-like cells (S). Embryonal mass lacks a protoderm-like layer (cf. Fig. 7A). The embryo is developmentally comparable to that shown in Fig. 4P. (B) Somatic embryo with a protoderm-like layer (PD) at the end of early embryogenesis (developmentally comparable to that shown in Fig. 6C, D). (C) Somatic embryo in the beginning-middle of late embryogenesis (developmentally comparable to that shown in Fig. 6E, F). The shape is rounded rather than elongated. The onset of histogenesis is still not evident (cf. Fig. 7C). (D) Somatic embryo with already differentiated but still not elongated cotyledons (C) at the end of late embryogenesis (developmentally comparable to that shown in Fig. 6G). Width of the embryo approximates its length. Root meristem (RM) is located closer to shoot apex (A) than in the A-type embryo counterpart (cf. Fig. 7D). EC, embryonal cortex; PC, procambium; RC, root cap. (E) Nearly mature somatic embryo with elongated cotyledons (C). Note the presence of air spaces close to shoot apex. (F) Enormously enlarged mature somatic embryo with disintegrated tissues (asterisks; cf. Fig. 7E). The embryo is developmentally comparable to that shown in Fig. 6H. Bars = 250 μ m.

sometime occurred soon after transdifferentiation, prior to the elongation of the suspensor (data not shown), although the main response of somatic embryos to ABA was their individual development to mature forms (Fig. 9).

The patterns of monoclonal antibody JIM13-labelling of proembryogenic masses and somatic embryos

There are many indications that AGPs have important roles in plant development (Kreuger and van Holst, 1996). The monoclonal antibody JIM13 was raised against the AGP fraction isolated from the conditioned medium of an embryogenic cell suspension of carrot (Knox *et al.*, 1991). In *P. abies*, a JIM13-reactive epitope was detected by immunoblotting samples of concentrated extracellular proteins from embryogenic cell suspensions (Egertsdotter and von Arnold, 1995). This raised the

question of whether the AGP recognized by JIM13 could be used as a marker of different stages of somatic embryogenesis in *P. abies*.

By using immunocytochemistry, it was found that the staining pattern with JIM13 was different between PEMs and somatic embryos. Proembryogenic masses had JIM13 positive material in the majority of their cell walls, throughout the whole region of small densely cytoplasmic and highly vacuolated cells (Fig. 10A–D). The highest expression of JIM13-reactive epitope was found in transdifferentiating PEM III (Fig. 10E, F). Interestingly, newly formed somatic embryos did not react with the antibody (Fig. 10E, F). In more developed somatic embryos, immunolabelling was restricted to a limited number of cells in the root cap and pith regions (Fig. 10G, H).




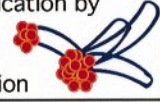




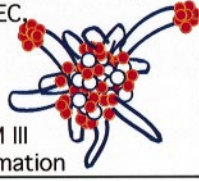



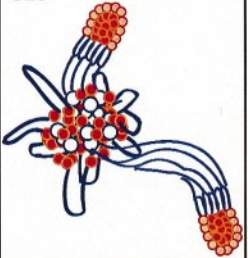




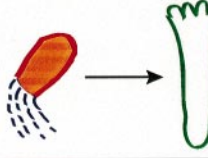

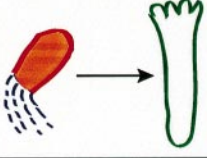
Initial structure	Number of structures analysed	Conditions			
		liquid medium		solidified medium	
		auxin + cytokinin	ABA	auxin + cytokinin	ABA
PEM I 	336	multiplication by UDEC 	death 	multiplication by UDEC, PEM II formation 	death 
PEM II 	618	multiplication by UDEC 	death 	multiplication by UDEC, PEM III formation 	death 
PEM III 	498	multiplication by UDEC 	transdifferentiation to SEs 	multiplication by UDEC 	transdifferentiation to SEs 
early SE 	256	proliferation of embryonal mass 	SE development 	proliferation of embryonal mass 	SE development 

Fig. 9. Comparison of developmental responses of PEMs and early somatic embryos under different conditions. The illustrated patterns are conclusions based on the analysis of a large number of PEMs and somatic embryos (shown in second column) placed either in liquid medium held in 24 well plates or in solidified medium in thin layers of agarose. 'Auxin and cytokinin' and 'ABA' refer to proliferation and maturation media, respectively. Proembryogenic masses and early somatic embryos were taken from proliferating suspension culture (cell line A95.88.22), 3 d and 7 d after subculture, respectively. The crude suspension culture was sieved through 200 μm nylon mesh for dissociation of adhered cell aggregates, and the $>200 \mu\text{m}$ fraction plated in 24 well plates or agarose layers with a low density (25–30 PEMs or somatic embryos ml^{-1}). Developmental responses were analysed 5 d after plating. Degradation of suspensor-like cells in early somatic embryos is shown by dotted lines. Cleavage-type multiplication of early somatic embryos observed sometimes in proliferation medium is not shown. SE, somatic embryo; UDEC, unequal division of embryogenic cells with dense cytoplasm.

Discussion

Comparison of somatic versus zygotic embryogenesis in *Picea abies*

The present study has shown that somatic embryogenesis of *P. abies* proceeds through a PEM-phase, followed by formation and development of somatic embryos. An important question to be answered is what are the common and different features held by zygotic versus somatic embryogenesis in *P. abies*.

Although the earliest stages of somatic embryo development comparable to proembryogeny could not be characterized, the subsequent developmental processes during somatic embryo patterning correspond closely to what

occurs in the course of early and late zygotic embryogeny (Singh, 1978). During early zygotic embryogeny, the embryonal mass enlarges and elongates mainly through periclinal division of cells in the proximal part of an embryo (Yeung *et al.*, 1998). Derivative cells elongate and contribute to the formation of a secondary suspensor (i.e. embryonal tubes). A protoderm-like cell layer arises through alternating peri- and anticlinal divisions in the distal part of an embryo. Histogenesis and differentiation of apical meristems occur during late embryogeny. At this time, the embryo can be arbitrarily divided into a micropylar part, where the root cap forms, and a chalazal part bearing the shoot meristem and involved in embryo elongation. A mature zygotic embryo in the Pinaceae has

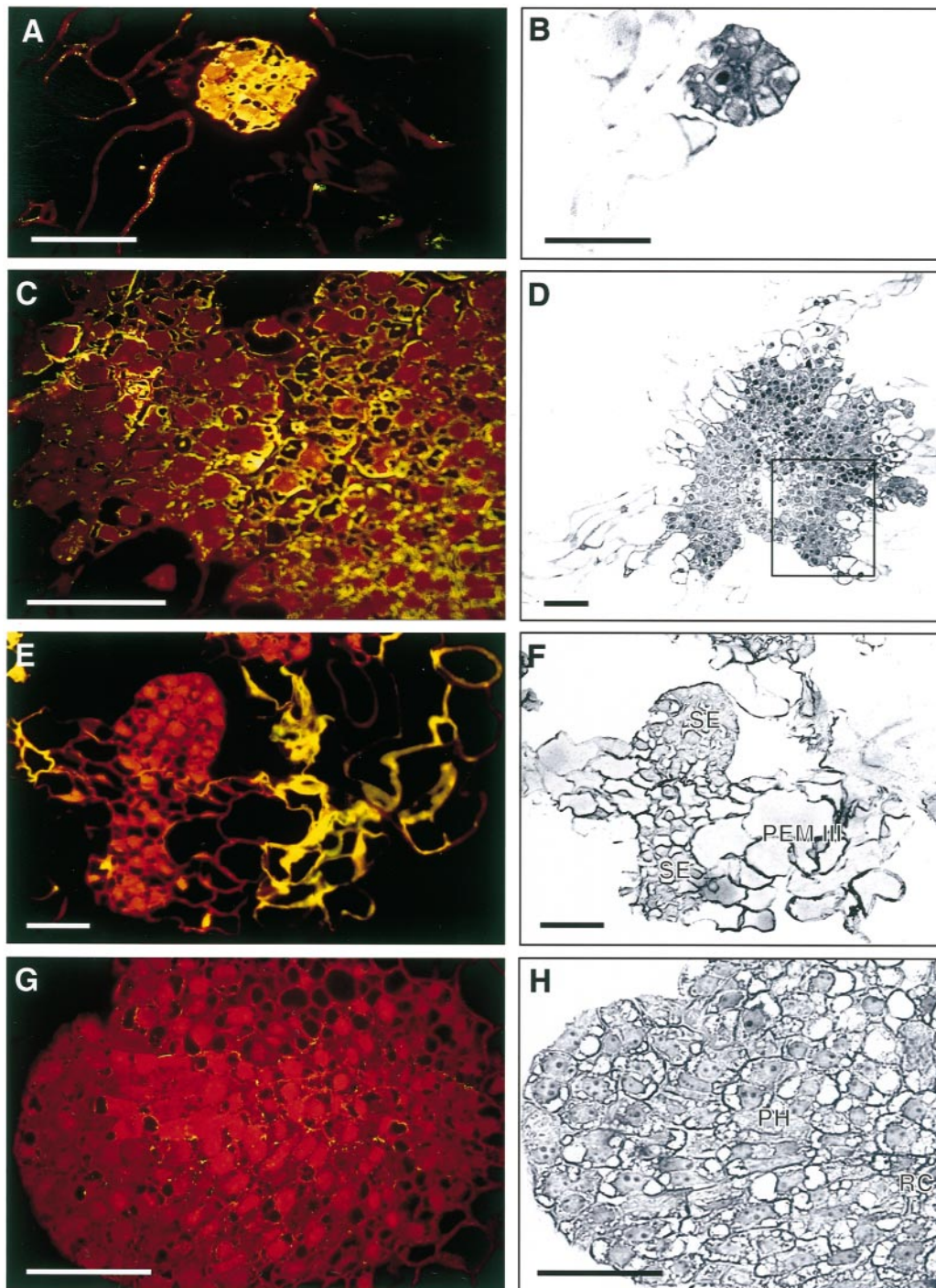


Fig. 10. Distribution of JIM13-reactive epitope of AGPs through PEM versus somatic embryo tissues. Immunolocalization of the epitope is represented by yellow to green fluorescence of cell walls. Autofluorescence of non-labelled cells is shown in dark red. (A, C, E, G), immunostained sections; (B, D, F, H), serial sections stained with toluidine blue. (A, B) Proembryogenic mass I taken 3 d after subculture of proliferating suspension culture (cell line B41). Abundant localization of the epitope throughout the whole region of small densely cytoplasmic cells. (C, D) Proembryogenic mass III taken 7 d after subculture of proliferating suspension culture (cell line B41). Both densely cytoplasmic and highly vacuolated cells are labelled with JIM13 at their cell walls. Immunostained region shown in (C) roughly corresponds to the area within the box in (D) rotated by 90°. (E, F) Representative example of transdifferentiation of PEM III to two somatic embryos (SE). The sample was taken 5 d after suspension culture (cell line A95.88.22) has been plated in ABA-containing agarose layer. The region of PEM III adjacent to somatic embryos, and comprised of enlarged cells with collapsed protoplasm, exhibits strong specific immunostaining, while somatic embryos derived from this PEM III do not react to the antibody. (G, H) Somatic embryo developing for 14 d in ABA-containing agarose layer (cell line A95.88.22). Note the weak localization of JIM13-reactive epitope in some cells of pith (PH) and root cap (RC). Bars = 100 μ m.

several cotyledons, a primary root and shoot meristem, and distinct procambium, cortex, pith, and root cap. The protoderm covers the shoot and hypocotyl region and ends abruptly at a junction zone between the root cap and hypocotyl (Singh, 1978). Somatic embryos of *P. abies* have a strikingly similar developmental pattern in the terms of temporal succession of histogenetic processes and spatial distribution of various tissues in the embryo body (Figs 5, 7). The only difference found between somatic and zygotic embryos of *P. abies* is related to cleavage polyembryony, which is in fact a peculiar natural feature of *Pinus*, rather than *Picea* (Chowdhury, 1962). Nevertheless, in embryogenic cultures *in vitro*, all 'non-cleavage' conifers (i.e. *Picea*, *Larix* and *Pseudotsuga*) commonly display cleavage polyembryony (for review see Attree and Fowke, 1993).

There are no fundamental differences between A- and B-group cell lines in the developmental pathways leading to somatic embryo formation, except for those B-lines in which the formation of somatic embryos is completely blocked (line B88.1 in the present study). In A-group somatic embryos, formation of the protoderm-like cell layer occurs early, in auxin-free medium, likewise in carrot (Emons, 1994). Somatic embryos of the B-group, however, lack protoderm until subjected to ABA-treatment. The ABA-stimulation of protoderm formation was also found in maize somatic embryos (Emons, 1994). The radial growth of the shoot part in A-group somatic embryos is suppressed at the end of late embryogeny, much as during zygotic embryogenesis of gymnosperms (Sterling, 1948). Intensive radial growth and delay in the onset of histogenesis displayed by B-embryos of *P. abies* were recently described for *in vitro*-cultured zygotic embryos of *Brassica juncea* treated with the auxin transport inhibitor *N*-(1-naphthyl)thalamic acid (Hadfi *et al.*, 1998). Therefore abnormal development of B-embryos during early and late embryogeny may be attributed to perturbations in endogenous polar auxin transport.

It is difficult to find any analogy to PEM in zygotic embryogenesis. A comparable stage might exist in the Pinaceae, where in zygotic embryos cells of the suspensor go through an abortive meristematic activity forming the group of cells called the 'rosette' tier (Singh, 1978). The products of continuous cell divisions in the 'rosette' tier were named 'rosette' embryos. Perhaps, one can make a comparison between PEM III giving rise to somatic embryos and the 'rosette' tier in Pinaceae zygotic embryogeny. However, this is only a phenotypic analogy, because the 'rosette' embryos represent irregular meristematic activity and have never been observed to give rise to a viable embryo (Berlyn, 1972), whereas PEM III cells are the source of developing somatic embryos. In this connection, the possibility that PEMs are actually early somatic embryos deviating widely from the normal pathway can not be ruled out.

The model for somatic embryogenesis in *Picea abies*

The embryogenic cell suspension of carrot is the most thoroughly studied embryogenic system, both at morphological and molecular levels (Fujimura and Komamine, 1980; Nomura and Komamine, 1985; Borkird *et al.*, 1988; de Vries *et al.*, 1988; Komamine *et al.*, 1990; Pennell *et al.*, 1992). Therefore, it is worthwhile to contrast the observations on *P. abies* from this study with the carrot model.

By using just a few morphological criteria (dimensions and shape of the cell, and density of cytoplasm), the single cells in carrot embryogenic suspension can be categorized into several groups (Nomura and Komamine, 1985; Toonen *et al.*, 1994). However, the content of cytoplasm was shown to be a major factor determining the embryogenic competence of single cells (Komamine *et al.*, 1990; Toonen *et al.*, 1994). Some authors therefore distinguish only two types of cell, densely cytoplasmic and highly vacuolated (Emons, 1994). In embryogenic cell suspensions of *P. abies*, double-staining with acetocarmine and Evan's blue allows both these types of cell to be distinguished, which constitute most multicellular aggregates. However, when a single cell fraction was obtained through fractionation of crude suspensions, neither densely cytoplasmic nor vacuolated cells on their own could develop into somatic embryos. In contrast, few-celled structures (i.e., PEMs I) of *P. abies* readily developed further and passed through all the consecutive stages up to formation of somatic embryos. This shows the importance of intercellular communication for acquisition and realization of embryogenic competence (Spangenberg *et al.*, 1985; de Vries *et al.*, 1988).

A model for somatic embryogenesis in *P. abies* is shown in Fig. 11. The whole pathway can be divided into three major steps: successive growth of the PEMs through the three stages, formation of somatic embryos from PEM III, and development of somatic embryos till maturity.

The PEM I formation through unequal division of embryogenic cells with dense cytoplasm is similar to the first division of carrot embryogenic cells giving rise to a small densely cytoplasmic apical cell and large vacuolated basal cell (Emons, 1994; Toonen *et al.*, 1994). The PEM I of *P. abies* is also comparable with state 1 cell clusters of carrot described previously (Komamine *et al.*, 1990). Both *P. abies* PEM I and carrot state 1 clusters multiply in liquid medium under continuous supply of auxin which inhibits their further development (Halperin, 1966; de Vries *et al.*, 1988; Toonen *et al.*, 1994). It is plausible that formation of PEM I could have been mistaken for real somatic embryo formation in conifers (i.e. second mechanism described in Introduction: formation of somatic embryos through an asymmetrical division of a single cell).

Partial or complete depletion of auxin permits growth

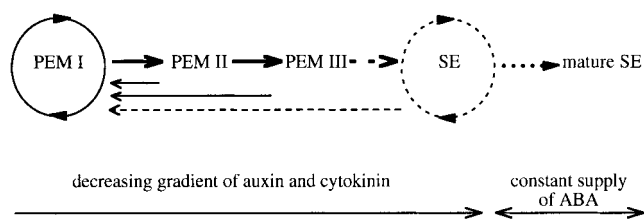


Fig. 11. The model for somatic embryogenesis in *Picea abies*. Closed solid line represents the cyclic process of multiplication at PEM I level by unequal division of embryogenic cells with dense cytoplasm. This process predominates under constant supply of auxin and cytokinin in liquid medium. When immobilization is applied and/or auxin and cytokinin are being gradually depleted, the average level of the whole system is biased forward, to PEM II or PEM III levels (bold solid lines). This occurs towards the end of a liquid culture passage or in callus culture. Once auxin-treatment has been applied to PEMs II or PEMs III (e.g. when cells are subcultured into fresh proliferation medium), the new PEMs I arise by unequal division of embryogenic cells from more developed PEMs (fine solid lines). Bold dashed line shows transdifferentiation of PEM III to somatic embryos. Those conditions which are inhibitory for PEM multiplication are stimulatory for transdifferentiation (e.g. depletion of auxin and cytokinin, immobilization, addition of ABA, etc). Sometime the process can be turned back, from somatic embryos to PEM I (fine dashed line). This occurs when the balance of factors which stimulate transdifferentiation is disturbed (see response of somatic embryos to proliferation conditions shown in Fig. 9). Somatic embryo level is maintained either by cleavage of early somatic embryos (closed dashed line) or through their development to mature forms (bold dotted line). Absciscic acid is especially required for the latter process.

of *P. abies* PEM I to more advanced stages, PEM II and PEM III (Fig. 11). Similarly, in carrot, state 1 cell clusters develop to state 2 clusters in auxin-free medium; PEM growth was also shown in cucumber embryogenic cultures (Komamine *et al.*, 1990; Kreuger *et al.*, 1996). Once auxin treatment has been applied to PEMs II or PEMs III (e.g. when cells are subcultured into fresh proliferation medium), the new PEMs I arise by unequal division of embryogenic cells from more developed PEMs (Fig. 11). It is plausible that this process was previously misinterpreted as one of the mechanisms of somatic embryo formation in conifers (i.e. third mechanism described in Introduction: direct formation of new somatic embryos from small meristematic cells within suspensor-like cells).

Somatic embryo formation takes place under conditions which are inhibitory for PEM multiplication (e.g. depletion of auxin, immobilization, addition of ABA, etc; Fig. 11). It is not yet clear how this process is initiated, although this can not occur unless a 'critical mass' of the PEM cells has been formed. This process is analogous to carrot somatic embryo formation under auxin-deprived conditions (Nomura and Komamine, 1985).

Somatic embryos continue to form either by cleavage of early somatic embryos (i.e. first mechanism described in Introduction) or by re-iterated progression through the PEM stages (Fig. 11). Contrary to angiosperms, exogenously supplied ABA is obligatory for somatic embryo maturation in conifers (Dunstan *et al.*, 1998).

Proembryogenic mass versus somatic embryo markers

It is evident that one can not identify PEMs in *Picea* embryogenic cultures by virtue of their phenotypical similarity to zygotic embryos. Although an early PEM of *P. abies* is a polar structure with elongated suspensor-like cells, a great interclonal variation of shape and cellular constitution of PEMs has been found. In contrast, somatic embryos are morphologically conservative structures, possessing a distinct protoderm-like cell layer (timing of differentiation is a cell line-dependent characteristic), embryonal tubes and suspensor-like cells.

The presence of specific epitopes of AGPs was shown to be an adequate marker for pinpointing transitional states during carrot somatic embryogenesis (Stacey *et al.*, 1990; Pennell *et al.*, 1992; McCabe *et al.*, 1997; Toonen *et al.*, 1997). In *P. abies*, somatic embryos can be clearly distinguished by the lack of staining of the AGP epitope recognized by the monoclonal antibody JIM13. The vast majority of PEM-cells expressed this epitope, but none of cells in the early somatic embryos. In more developed somatic embryos, the presence of the JIM13-reactive epitope was scarce and restricted to particular zones (i.e. root cap and pith).

There is increasing evidence that structural differentiation, cell proliferation and programmed cell death are functionally related and co-ordinated mechanisms ensuring maintenance of homeostasis in biological systems (Rinkenberger and Korsmeyer, 1997). It is tempting to speculate that the abundant accumulation of JIM13-reactive epitope of AGPs in PEMs III of *P. abies* is related to programmed cell death in PEM III upon transdifferentiation to somatic embryos. This idea is supported by the fact that the presence of the same AGP epitope in the cells of maize coleoptiles and zinnia mesophyll has been shown to be related to programmed cell death during xylem transdifferentiation (Schindler *et al.*, 1995; Stacey *et al.*, 1995). Further studies will be aimed at testing this hypothesis by combining cell tracking techniques and molecular markers for programmed cell death.

Acknowledgements

We gratefully acknowledge Dr Keith Roberts (John Innes Centre, Norwich, UK) for his kind gift of the JIM13 monoclonal antibody, Dr Roland Grönroos for generous help with art work and Dr David Clapham for critical reading of the manuscript. The research was supported by Thematic research project (joint Swedish University of Agricultural Sciences/the Forestry Research Institute of Sweden) and the Centre for Forest Biotechnology.

References

- Attree SM, Fowke LC. 1993. Embryogeny of gymnosperms: advances in synthetic seed technology of conifers. *Plant Cell, Tissue and Organ Culture* **35**, 1–35.

- Backs-Hüsemann D, Reinert J.** 1970. Embryobildung durch isolierte Einzelzellen aus Gewebekulturen von *Daucus carota*. *Protoplasma* **70**, 49–60.
- Baskin TI, Busby CH, Fowke LC, Sammut M, Gubler F.** 1992. Improvements in immunostaining samples embedded in methacrylate: localization of microtubules and other antigens throughout developing organs in plants of diverse taxa. *Planta* **187**, 405–413.
- Berlyn GP.** 1972. Seed maturation and germination. In: Kozłowski TT, ed. *Seed biology* I. New York: Academic Press, 223–312.
- Borkird C, Choi JH, Jin Z, Franz G, Hatzopoulos P, Chorneau R, Bonas R, Pelegri F, Sung ZR.** 1988. Developmental regulation of embryonic genes in plants. *Proceedings of the National Academy of Sciences, USA* **85**, 6399–6403.
- Chowdhury CR.** 1962. The embryogeny of conifers: a review. *Phytomorphology* **12**, 313–338.
- de Vries SC, Booij H, Meyerink P, Huisman G, Wilde DH, Thomas TL, van Kammen A.** 1988. Acquisition of embryogenic potential in carrot cell-suspension culture. *Planta* **176**, 196–204.
- Dong J-Z, Dunstan DI.** 1994. Growth parameters, protein and DNA synthesis of an embryogenic suspension culture of white spruce (*Picea glauca*). *Journal of Plant Physiology* **144**, 201–208.
- Dunstan DI, Dong J-Z, Carrier DJ, Abrams SR.** 1998. Events following ABA treatment of spruce somatic embryos. In *Vitro Cellular Developmental Biology* **34P**, 159–168.
- Egertsdotter U, von Arnold S.** 1993. Classification of embryogenic cell lines of *Picea abies* as regards protoplast isolation and culture. *Journal of Plant Physiology* **141**, 222–229.
- Egertsdotter U, von Arnold S.** 1995. Importance of arabinogalactan proteins for the development of somatic embryos of Norway spruce (*Picea abies*). *Physiologia Plantarum* **93**, 334–345.
- Egertsdotter U, von Arnold S.** 1998. Development of somatic embryos in Norway spruce. *Journal of Experimental Botany* **49**, 155–162.
- Egertsdotter U, Mo LH, von Arnold S.** 1993. Extracellular proteins in embryogenic suspension cultures of Norway spruce (*Picea abies*). *Physiologia Plantarum* **88**, 315–321.
- Emons AMC.** 1994. Somatic embryogenesis: cell biological aspects. *Acta Botanica Neerlandica* **43**, 1–14.
- Fujimura T, Komamine A.** 1980. The serial observation of embryogenesis in a carrot cell suspension culture. *New Phytologist* **86**, 213–218.
- Golds TJ, Babczinsky J, Rauscher G, Koop H-U.** 1992. Computer-controlled tracking of single cell development in *Nicotiana tabacum* L. and *Hordeum vulgare* L. protoplasts embedded in agarose/alginate films. *Journal of Plant Physiology* **140**, 582–587.
- Gubler F.** 1989. Immunofluorescence localization of microtubules in plant root tips embedded in butyl-methyl methacrylate. *Cell Biology International Reports* **13**, 137–145.
- Hadfi K, Speth V, Neuhaus G.** 1998. Auxin-induced developmental patterns in *Brassica juncea* embryos. *Development* **125**, 879–887.
- Halperin W.** 1966. Alternative morphogenetic events in cell suspensions. *American Journal of Botany* **53**, 443–453.
- Irish VF, Sussex IM.** 1992. A fate map of the *Arabidopsis* embryonic shoot apical meristem. *Development* **115**, 745–753.
- Knox JP, Linstead PJ, Peart J, Cooper C, Roberts K.** 1991. Developmentally regulated epitopes of cell surface arabinogalactan proteins and their relation to root tissue pattern formation. *The Plant Journal* **1**, 317–326.
- Komamine A, Matsumoto M, Tsukahara M, Fujiwara A, Kawahara R, Ito M, Smith J, Nomura K, Fujimura T.** 1990. Mechanisms of somatic embryogenesis in cell cultures—physiology, biochemistry and molecular biology. In: Nijkamp HJJ, Van der Plas LHW, Van Aartrijk J, eds. *Progress in plant cellular and molecular biology*. The Netherlands: Kluwer Academic Publishers, 307–313.
- Kreuger M, van der Meer W, Postma E, Abbestee R, Raaijmakers N, van Holst G-J.** 1996. Genetically stable cell lines of cucumber for the large-scale production of diploid somatic embryos. *Physiologia Plantarum* **97**, 303–310.
- Kreuger M, van Holst G-J.** 1996. Arabinogalactan proteins and plant differentiation. *Plant Molecular Biology* **30**, 1077–1086.
- Krogstrup P.** 1986. Embryo-like structures from cotyledons and ripe embryos of Norway spruce (*Picea abies*). *Canadian Journal of Forest Research* **16**, 664–668.
- McCabe PF, Valentine TA, Forsberg LS, Pennell RI.** 1997. Soluble signals from cells identified at the cell wall establish a developmental pathway in carrot. *The Plant Cell* **9**, 2225–2241.
- Mo LH, Egertsdotter U, von Arnold S.** 1996. Secretion of specific extracellular proteins by somatic embryos of *Picea abies* is dependent on embryo morphology. *Annals of Botany* **77**, 143–152.
- Mordhorst AP, Toonen MA, de Vries SC.** 1997. Plant embryogenesis. *Critical Reviews in Plant Sciences* **16**, 535–576.
- Nomura K, Komamine A.** 1985. Identification and isolation of single cells that produce somatic embryos at a high frequency in a carrot suspension culture. *Plant Physiology* **79**, 988–991.
- Pennell RI, Janniche L, Scofield GN, Booij H, de Vries SC, Roberts K.** 1992. Identification of a transitional cell state in the developmental pathway to carrot somatic embryogenesis. *Journal of Cell Biology* **119**, 1371–1380.
- Rinkenberger JL, Korsmeyer SJ.** 1997. Errors of homeostasis and deregulated apoptosis. *Current Opinions in Genetics and Development* **7**, 589–596.
- Schindler T, Bergfeld R, Schopfer P.** 1995. Arabinogalactan proteins in maize coleoptiles: developmental relationship to cell death during xylem differentiation but not to extension growth. *The Plant Journal* **7**, 25–36.
- Singh H.** 1978. *Embryology of gymnosperms*. Berlin: Borntrager.
- Spangenberg G, Koop H-U, Schweiger H-G.** 1985. Different types of protoplasts from *Brassica napus* L.: analysis of conditioning effects at the single cell level. *European Journal of Cell Biology* **39**, 41–45.
- Stacey NJ, Roberts K, Carpita NC, Wells B, McCann MC.** 1995. Dynamic changes in cell surface molecules are very early events in the differentiation of mesophyll cells from *Zinnia elegans* into tracheary elements. *The Plant Journal* **8**, 891–906.
- Stacey NJ, Roberts K, Knox JP.** 1990. Patterns of expression of the JIM 4 arabinogalactan-protein epitope in cell cultures and during somatic embryogenesis in *Daucus carota* L. *Planta* **180**, 285–292.
- Sterling C.** 1948. Proembryo and early embryogeny in *Taxus cuspidata*. *Bulletin of the Torrey Botanical Club* **75**, 469–485.
- Strehlow D, Gilbert W.** 1993. A fate map for the first cleavage of zebrafish. *Nature* **361**, 451–453.
- Toonen MAJ, Hendriks T, Schmidt EDL, Verhoeven HA, van Kammen A, de Vries SC.** 1994. Description of somatic-embryo-forming single cells in carrot suspension cultures employing video cell tracking. *Planta* **194**, 565–572.
- Toonen MAJ, Schmidt EDL, Van Kammen A, De Vries SC.** 1997. Promotive and inhibitory effects of diverse arabinogalactan proteins on *Daucus carota* L. somatic embryogenesis. *Planta* **203**, 188–195.

- Tsukahara M, Komamine A.** 1997. Separation and analysis of cell types involved in early stages of carrot somatic embryogenesis. *Plant Cell, Tissue and Organ Culture* **47**, 145–151.
- von Arnold S, Eriksson T.** 1981. In vitro studies of adventitious shoot formation in *Pinus contorta*. *Canadian Journal of Botany* **59**, 870–874.
- von Arnold S, Hakman I.** 1988. Plantlet regeneration *in vitro* via adventitious buds and somatic embryos in Norway spruce (*Picea abies*). In: Hanover JW, Keathley DE, eds. *Genetic manipulation of woody plants*. New York: Plenum Press, 199–215.
- Yeung EC, Stasolla C, Kong L.** 1998. Apical meristem formation during zygotic embryo development of white spruce. *Canadian Journal of Botany* **76**, 751–761.
- Zimmerman JL.** 1993. Somatic embryogenesis: a model for early development in higher plants. *The Plant Cell* **5**, 1411–1423.